BORATE GLASSES, CRYSTALS & MELTS

Edited by:

Adrian C. WRIGHT, Steven A. FELLER and Alex C. HANNON

The Society of Glass Technology
Sheffield,1997

BORATE STRUCTURES BY VIBRATIONAL SPECTROSCOPY

Georgios D. CHRYSSIKOS & Efstratios I. KAMITSOS
Theoretical and Physical Chemistry Institute,
National Hellenic Research Foundation,
48 Vass. Constantinou Ave., Athens 11635, Greece

This paper deals with some recent contributions of infrared and Raman spectroscopies to the structural description of borate systems. It demonstrates how the vibrational spectra can assist the decoding of local and intermediate range structure of crystals and glasses. Spectroscopic tools have been developed to tackle thermodynamic and kinetic aspects of chemical reactions relevant to the vitrification of borates. Case studies of alkali and alkaline earth borate glasses and crystals highlight the cation and composition dependence of borate networks. The interactions between the network sites and the modifying cations are monitored by the characteristic cation motion bands in the far-infrared. Some structural aspects of the mixed-alkali effect are discussed.

1. INTRODUCTION

Borates with the general formula $xM_{2/n}O.(1-x)B_2O_3$ result commonly from the fusion of boric anhydride, B_2O_3, with metal oxides $M_{2/n}O$ provided by the thermal decomposition of carbonate or nitrate salts. The structural chemistry of borates is very rich, and their phase diagrams include broad glass-forming ranges. There is an extensive research effort aiming at the elucidation, classification, and prediction of borate structures, much of which relies on vibrational spectroscopic techniques.

The purpose of this report is to highlight contributions of vibrational spectroscopy to the systematic structural mapping of borate crystals and glasses by presenting selective spectroscopic tools and structural concepts employed in the authors' laboratory over the last decade. The principles and instrumentation of infrared and Raman spectroscopies can be found in books and monographs. Technical details, spectral analysis and band assignments should be sought in the original references.

2. THE LOCAL STRUCTURE OF BORATE NETWORKS

Boron has an s^2p^1 electronic configuration. In borates it adopts sp^2 or sp^3 hybridizations, therefore acquiring trigonal or tetrahedral coordination. In the former case boron affords an empty p_z orbital perpendicular to the borate plane. The planarity of the borate triangle is enhanced by the π-bonding between this

Table 1
Schematic structural classification of borate polyhedra as a function of stoichiometry

$xM_{2/n}O.(1-x)B_2O_3$		Average stoichiometry	Local structure 3-coordinated		4-coordinated	
0		$BO_{1.5}^{0}$	$B\emptyset_3^0$	Ref. [2]		
0·5	meta	BO_2^{1-}	$B\emptyset_2O^{1-}$	Ref. [3]	$B\emptyset_4^{1-}$	Ref. [4]
0·67	pyro	$BO_{2.5}^{2-}$	$B\emptyset O_2^{2-}$	Ref. [5]		
0·75	ortho	BO_3^{3-}	BO_3^{3-}	Ref. [6]	$B\emptyset_2O_2^{3-}$	Ref. [9]
0·83	5:1	BO_4^{5-}			BO_4^{5-}	Ref. [7]

empty p_z orbital and the filled p orbitals of the (bridging and non-bridging) oxide ligands [1]. Alternatively, the σ nucleophilic attack of oxygens lying above or below the plane, leads to the formation of 4-coordinated borate species.

Table 1 comprises a list of the network polyhedra found in borate compounds as a function of stoichiometry. Oxygen atoms are shown either bridging two boron centers (Ø), or as non-bridging or terminal (O). There is direct crystallographic evidence for all species [2-7], except for the 4-coordinated orthoborate ($B\emptyset_2O_2^{3-}$), analogous to $Al\emptyset_2O_2^{3-}$ [8], for which the only evidence comes from the interpretation of the Raman spectrum of some alkali orthoborate glasses [9]. Polyhedra with oxygen coordinated to three boron centers [10] are not included in Table 1.

To a good approximation, the polyhedra of Table 1 can be considered as the primary building blocks for every borate structure, either glassy or crystalline. For example, diborate crystals and glasses, with average stoichiometry (x=0·33) not corresponding to that of a primary polyhedron, ought to consist of formally neutral $B\emptyset_3^0$ triangles and metaborate polyhedra ($B\emptyset_2O^{1-}$ triangles and/or $B\emptyset_4^{1-}$ tetrahedra) in equal proportions. There are two chemical processes leading to structural diversification at the local level. The first is the *isomerization* between 3- and 4-coordinated species of the same stoichiometry (e.g. $B\emptyset_2O^{1-} \Leftrightarrow B\emptyset_4^{1-}$), the second is the *disproportionation* of a species into polyhedra of higher and lower stoichiometry (e.g. $2B\emptyset O_2^{2-} \Leftrightarrow B\emptyset_2O^{1-} + BO_3^{3-}$). Both depend on the nature of the M^{n+} cation [9,11].

The species of Table 1 have distinct vibrational signatures due to differences in symmetry and bonding. Despite the fact that these signatures can be obscured by the coupling between different groups, crystal field effects, or merely by the coexistence of many groups with overlapping spectra, the spectroscopic identification of the local structural species is in many cases possible [12, 13]. As an example, Fig. 1 compiles the infrared absorption spectra of representative $xLi_2O.(1-x)B_2O_3$ glasses with compositions spanning the glass forming range. The spectra are collected in the specular reflectance mode which ensures continuous spectral acquisition over broad frequency ranges (30-4000 cm^{-1}) and yields quantitative spectra free of hydrolysis and optical dispersion effects [14]. While detailed assignments are provided in [14], we note here that the stretching vibrations of metaborate tetrahedra, $B\emptyset_4^{1-}$, are observed at fre-

quencies (800-1100 cm^{-1}) lower than the corresponding modes of borate triangles (1100-1600 cm^{-1}). Analysis of the spectra and appropriate ratioing of integrated intensities, (Fig. 2a), demonstrates the non-monotonic dependence of the fraction of four-coordinated boron centers in the glass (N_4) on x [14], already familiar from the NMR work of P. J. Bray [15], as well as the composition dependence of meta-, pyro- and orthoborate triangles. The same spectral features allow the determination and quantification of a pronounced cation dependence of N_4 [16], where for a fixed stoichiometry below the metaborate, the larger alkalis induce the formation of fewer tetrahedral species and, consequently, favor increased fractions of $B\emptyset_2O^{1-}$ triangles [13, 16, 17] (Figure 2b). Incidentally, this trend appears reversed for x>0·50 [9].

3. DANGLING BONDS ON BORATE TRIANGLES: A RAMAN PROBE OF INTERMEDIATE ORDER

Let us now focus on the distribution of π-bonding over the three B–O bonds of a borate triangle. The three oxygen atoms will compete for the empty boron p_z orbital and their ability to neutralize boron will depend on their charge (basicity) and on how much of this charge is involved in bonding outside the triangle, i.e. towards the neighboring boron centers and/or towards the charge balancing cations M^{n+}. Therefore, in the general case, the three B–O bonds of the triangle will be of unequal length and strength, (i.e. of unequal force constant), and would result in different B–O stretching frequencies. All of these are valid strictly

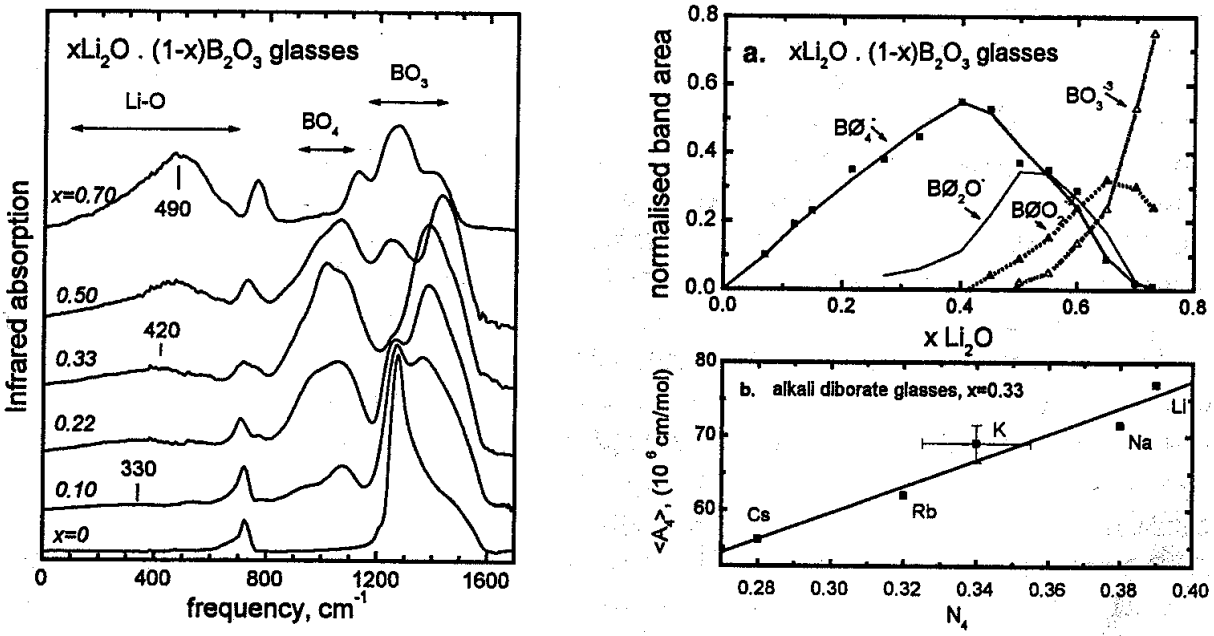

Fig.1. (left) Infrared absorption spectra of selected $xLi_2O.(1-x)B_2O_3$ glasses [14]
Fig. 2. (right) **(a)** Compositional dependence of the integrated intensities of infrared bands due to metaborate tetrahedra and meta-, pyro, and orthoborate triangles in lithium borate glasses. Lines are guiding the eye [14]. **(b)** Cation dependence of the integrated intensity of the infrared envelope due to $B\emptyset_4^{1-}$ units in alkali diborate glasses. The line is a linear least squares fit [16].

in the dipole approximation. The structural entity that most closely fulfills the requirement for vibrational decoupling from the rest of the network is the B–O^- dangling bond, especially when the charge balancing M–O interactions are fully ionic and, therefore, weak. Due to its large force constant, the stretching vibration of these B–O^- bonds is observed in the highest frequency part of the Raman spectrum with very little interference from other vibrations. By the same token, it is often possible to locate at lower frequencies a strong feature that could be assigned to a stretching vibration of B–Ø bonds [18 and Refs. therein].

Based on the Raman spectra of nine meta-, pyro- and orthoborate crystals consisting solely of triangular units, a simple linear correlation has been developed between the boron–oxygen bond length, (r), and the corresponding stretching frequency ν in cm^{-1}, ν=16900–11600r, (1·31≤r≤1·40 Å). Since r has been empirically correlated with the valence of the B–O bond, s, the latter can be correlated also with ν: s=0·8+2×$10^{-4}\nu$. The implications (and limitations) of the two equations have been presented elsewhere [18]. We only note here that spectral acquisition at ±2 cm^{-1} accuracy in reading band maxima allows Raman spectroscopy to monitor minute changes of r or s in borate triangles. Such changes often result from second neighbor effects (i.e. from intermediate range order).

Representative Raman signatures of metaborate B–O^- triangles in crystals and glasses are shown in Fig. 3. Crystalline $NaBO_2$ and α-$LiBO_2$ consist solely of metaborate triangles. The large frequency difference of their B–O^- stretches (ca. 1560 cm^{-1} vs. 1485 cm^{-1}) reflects their different intermediate range order: rings vs. chains [19]. The presence of two basic $B\emptyset_4^-$ units adjacent to the $B\emptyset_2O^-$ "probe" in $Ba_2LiB_5O_{10}$ strengthens the B–Ø bonds of the triangle and shifts the B–O^- stretch to ca. 1400 cm^{-1} [18]. Even lower frequencies (ca. 1360 cm^{-1}) are measured in crystalline Li_2BAlO_4, where even more basic $Al\emptyset_4^-$ tetrahedra are neighboring the $B\emptyset_2O^-$ triangle [20]. Overall, the ca. 200 cm^{-1} frequency span of the metaborate B–O^- stretch corresponds approximately to a 0·02 Å variation in bond length and a 0·04 change in bond valence [18].

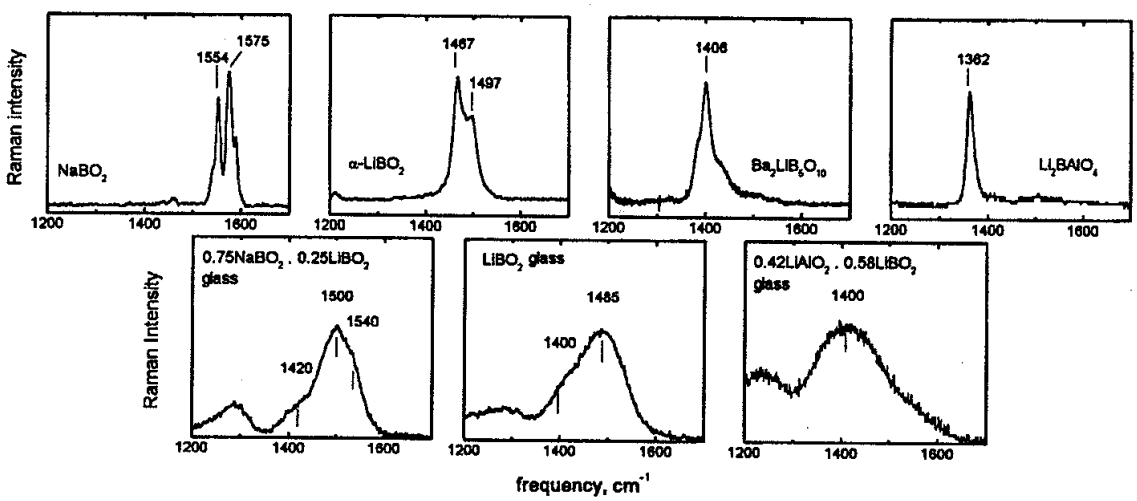

Fig.3. Raman spectra of B–O^- stretches in crystalline (top) and glassy (bottom) metaborates [18-20].

Based on this "calibration", we can now reveal the structural richness of metaborate glasses. For example, $B\emptyset_2O^-$ participates in (and probes) two distinct environments in glassy $LiBO_2$, [18] (see Fig. 3), a result confirmed by NQR [21]. These environments change systematically upon partial substitution of Li by Na, and of B by Al, and provide a structural fingerprint of the mixed alkali and mixed network effects [20,22]. Even more so, due to isomerization and disproportionation, the formation of metaborate triangles is not restricted to the metaborate stoichiometry. Thus, the $B–O^-$ stretch of $B\emptyset_2O^-$ units can be used to monitor the sequence of network polyhedra in every borate glass family, and over practically the whole glass forming range.

4. BORATE STRUCTURE AT INTERMEDIATE RANGES: RINGS, CONDENSED RINGS AND CHAINS

The primary polyhedra of Table 1 are not randomly connected in forming borate networks. Crystalline borate structures offer a variety of examples where these polyhedra are stabilized (mostly due to charge delocalization) in well-defined six-membered rings, condensed rings and chains [2,3,23-30].

Figure 4 compiles such structures built of $B\emptyset_3^0$, $B\emptyset_2O^-$, as well as $B\emptyset_4^-$ polyhedra. Isomerism is evident, especially for x=0·50, while the structural similarity between arrangements of different stoichiometry warrants easy disproportionations. Taking into account the charge balancing cations M^{n+}, the intermediate spatial order of these units is in the range of 5-10 Å. We also note that pyro- and orthoborate triangles which would lead to the cleavage of the arrangements of Fig. 4, can also form ring structures where the charge balancing cation M^{n+} occupies the place of a boron center [31].

As a rule of thumb, triangular borate network rings like the boroxol and the metaborate (see Fig. 4) have aromatic character. They tend to be planar and are stacked parallel to each other. This planarity is interrupted by four-coordinated boron atoms. Some crystalline compounds offer examples of intermediate cases where small deviations from planarity are due to weak B–O interplanar interac-

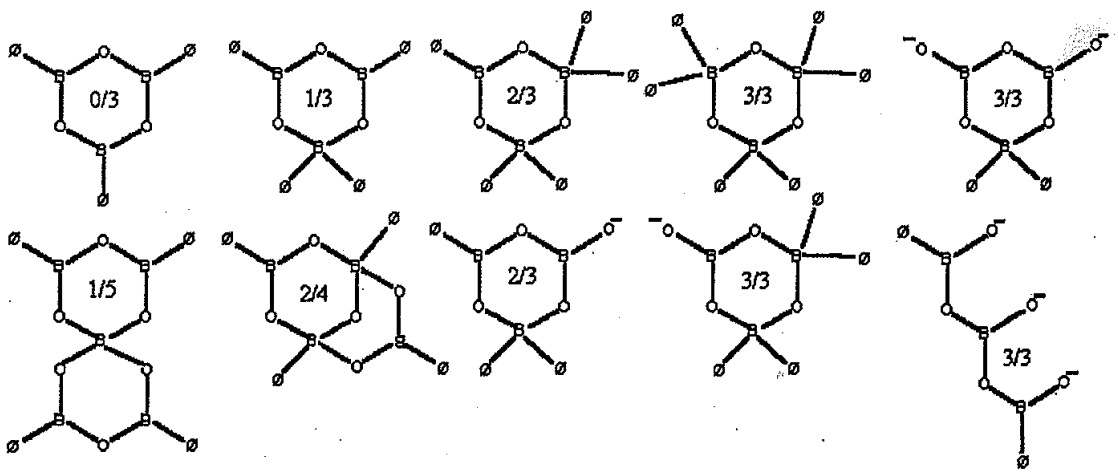

Fig. 4. Six-membered rings, condensed rings and chains found in crystalline borates. The labels denote their average formal negative charge per boron center, x/(1–x).

tions, precursing the isomerization of metaborate triangles into tetrahedra.

Due to differences in symmetry and bonding, the structures in Fig. 4 have discrete vibrational signatures which in many cases compare favorably with the predictions of group theory. Most structures of Fig. 4 exhibit breathing modes of the oxygen atoms which, due to the large polarisability changes involved, have strong Raman activity. It is on the basis of such a Raman band at 806 cm^{-1} that boroxol rings have been unambiguously identified as a major constituent of glassy B_2O_3 [32].

A more recent example of the extreme sensitivity of Raman spectroscopy to probe subtle structural differences of intermediate range order in borates is shown in Fig. 5. High temperature $NaBO_2$, BaB_2O_4 and CaB_2O_4 compounds are representative of three classes of metaborates which consist solely of $B\emptyset_2O^{1-}$ triangles but differ in their intermediate range ordering (D_{3h} aromatic rings with degenerate annular bonds, C_{3h} Kékulé rings and infinite chains, respectively) [19]. The Raman spectra probe the subtle cation-dependent structural difference between the ring structures which has occasionally remained unnoticed by crystallographers. Even more so, a correlation between spectroscopic parameters and the field strength of the charge balancing M^{n+} ion has guided the discovery of a hitherto unknown strontium metaborate compound with the C_{3h} ring structure [19].

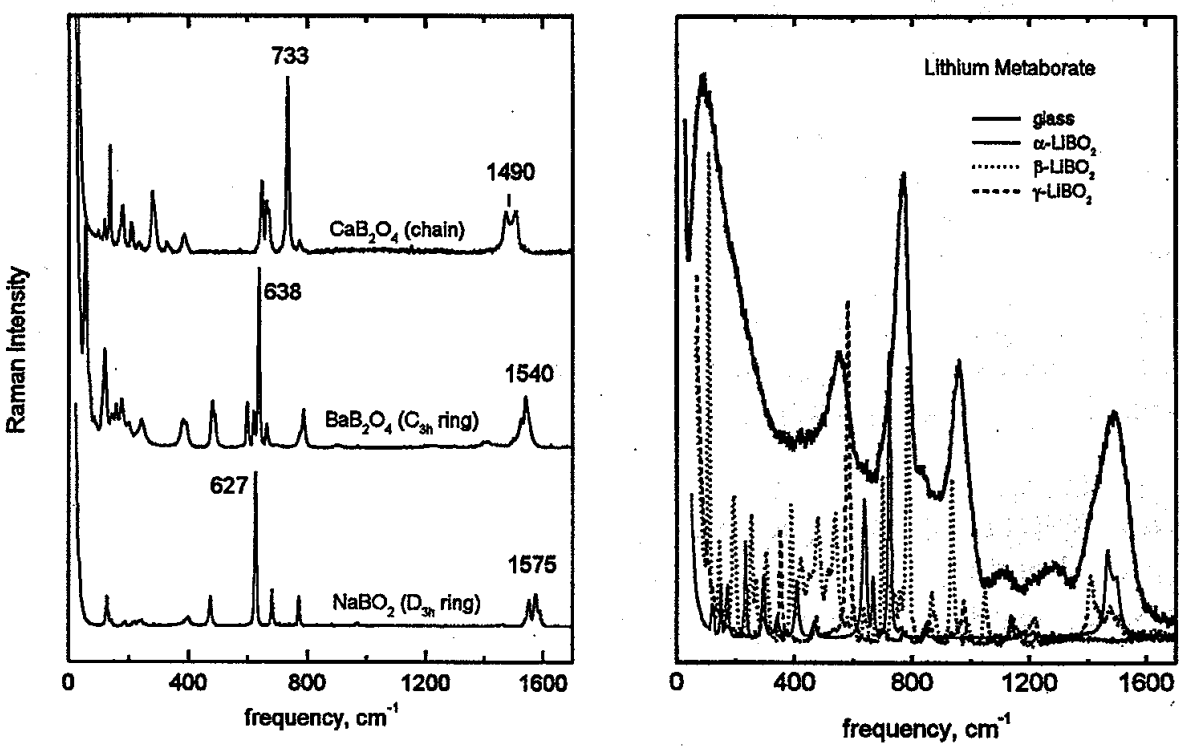

Fig. 5. (leftt) Raman spectra of CaB_2O_4, BaB_2O_4, and $NaBO_2$ crystals which consist of metaborate triangles [19].

Fig. 6. (left) Raman spectra of glassy lithium metaborate (thick solid line) as well as α- (thin solid line), β'- (dotted) and γ-$LiBO_2$ (dashed) polymorphs [35].

5. POLYMORPHISM AND GLASS FORMATION: LONGER RANGE STRUCTURE

Since Krogh-Moe [33] and Konijnendijk [34] conducted their studies, the comparative analysis of the vibrational spectra of glasses and compounds of crystallographically known structure has become a very useful method in assessing the structure of the former. A practical problem arises concerning the criterion in selecting those crystalline compounds that are of relevance to the composition of the glass under investigation. The available data basis of borate crystals favors high temperature congruent phases. Yet, forming a glass by melt cooling, involves the activation of temperature dependent chemical equilibria and their freezing close to the glass transition temperature.

It has been demonstrated that our knowledge of low temperature or incongruent phases can be enlarged by subjecting the glass to systematic low-temperature devitrification treatments [22,35]. In those cases where low temperature nucleation and crystallization occurs homogeneously, a relevance between the structure of the glass and those of the crystalline polymorphs is implied, and confirmed by spectral comparisons. Figure 6 provides an example of this comparison depicting the Raman spectrum of lithium metaborate glass together with the spectra of the three corresponding crystalline polymorphs. More interestingly, apart from the well known high temperature chain polymorph (α-$LiBO_2$), two tetrahedra-containing low-temperature polymorphs (β'-, and γ-$LiBO_2$), previously considered as high pressure phases, have been isolated by sub-T_g devitrification. Spectral comparison demonstrates that the glass exhibits structural similarities with its devitrification products, which extend beyond local and intermediate ranges [35].

It is tempting to interpret such data as suggesting that the structure of borate glasses can be inhomogeneous, in the sense that, relatively denser (tetrahedra containing low-temperature-like) domains seem to coexist with less dense (structurally metastable but kinetically arrested) liquid-like regions [35]. The sudden formation of the former upon quenching would cause a positive deviation of viscosity from Arrhenian behavior [36], and would therefore signal "fragility" in Angell's classification of glassforming liquids [37].

6. M–O INTERACTIONS IN BORATE GLASSES: GLASS MODIFIERS OR CONDITIONAL FORMERS?

B–O bonding yields only one part of the structural landscape of borate systems, the other being the M–O interactions. In fact, M and B coexist in the structure and compete for the negative charge of the oxide ions in a manner that depends on their relative concentration (i.e. on the composition of the system), and on the nature of M^{n+}. Obviously, M–O bonding as a structure determining factor becomes more important as the $M_{2/n}O$ fraction in the binary system increases. But is this only due to the fact that the M^{n+} cations outnumber the B^{3+} centers, or is there a manifestation for a qualitative change of M–O bonding with increasing $M_{2/n}O$ content?

The infrared spectra of $xLi_2O.(1-x)B_2O_3$ glasses shown in Fig. 1 can provide an answer to this question [14]. The absorption envelope of the spectra, dominating the far-infrared range below 550 cm^{-1}, has been shown to involve "rattling" vibrations of the Li^+ ion in the sites provided by the network. Such vibrations are observed in all modified glasses, with characteristic frequencies, widths and intensities depending on the mass of the cation M^{n+}, the nature of the glass former, and the composition [38]. While the details of the far-infrared spectroscopic study of glasses are beyond the scope of this report, we note in Fig. 1 that increasing x causes, apart from the expected increase of the band intensity, a systematic upward frequency shift of the Li–O vibrational mode. This latter trend is a direct manifestation of the enhancement of Li–O bond strength in glass [14], and therefore of increased Li–O covalency [39]. Indeed, the term "ionic modifier" describing the structural role of Li_2O in borate glasses ought to be used with caution for compositions of very high x.

Extending this thought to other M^{n+} cations, we show in Fig. 7 the x dependence of T_g in alkali and alkaline earth borates with $x<0{\cdot}50$ [40]. The bell shaped trend in all systems is associated with the non monotonic variation of the number of B–Ø bonds [16], due to the formation and the disappearance of $BØ_4^-$ species. Among alkali borates with $x<0{\cdot}50$, the Li-system has the highest T_g because it has the highest N_4. The glassy network of alkali borates is set mainly by freezing the boron–oxygen bonding; M_2O is therefore a modifier. In alkaline earth borates, increasing cationic field strength induces the increase of T_g, despite the *decrease* of N_4 [40,41]. Due to the high cross-linking efficiency of the M^{2+} ions, it is M–O bonding that freezes the glass structure before the formation of $BØ_4^-$ units, the low temperature choice of the B–O system, can be sufficiently activated. The oxides of the lighter alkaline earths act more as conditional glass formers [40,41].

A closer look at the far-infrared spectra reveals that they are asymmetric in a way that suggests a bimodal gaussian distribution of oscillators (Fig. 8) [16]. This is a general property of ionically modified glasses, although the relative intensity of the two components is cation- and, to some extent, composition-dependent. This bimodal nature of the far-infrared envelope has been associated with the existence of two distributions of cation-hosting environments in glass [41,42]. The high frequency component, is attributed to cation-site interactions bearing a higher degree of covalency, similar to those encountered in the relevant crystals. Cations that upon quenching do not succeed in achieving such environments assume more ionic (i.e. less basic) sites in the network [39]. Obviously, this interpretation is compatible with the concept of a microheterogeneous glass structure [35,43].

7. ON THE STRUCTURAL ASPECTS OF THE MIXED ALKALI EFFECT

The simultaneous presence of two modifying oxides induces a non-linear variation of dynamic glass properties on composition, which is known as the mixed mobile ion or mixed alkali effect (MAE) [44]. Most of the earlier theo-

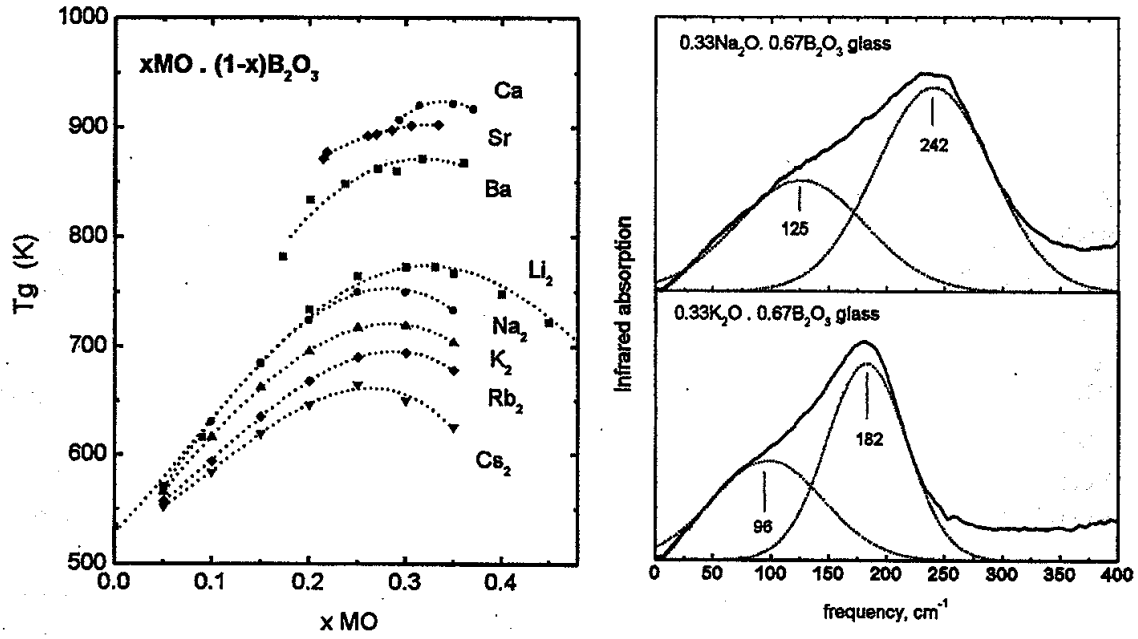

Fig. 7. (right) Glass transition temperatures of alkali and alkaline earth borate glasses [40].
Fig. 8. (left) Far-infrared spectra of Na-, and K-diborate glasses. Dotted lines show their deconvolution into Gaussian components [16,38].

ries accounting for the MAE were not concerned with the possibility of non-linear variations of the network structure upon alkali mixing.

It is quite evident from the vibrational [22,45-47] (as well as from the ^{11}B NMR [17]) spectra of mixed alkali borates below the metaborate composition, that alkali mixing causes the partial destruction of $B\emptyset_4^-$ groups and favors the formation of their triangular $B\emptyset_2O^-$ isomers (see Fig. 9). Also, in the presence of two alkalis, the crystallization and devitrification chemistry of borates is affected in a non-linear way [19,22]. Thus, alkali mixing affects the local and intermediate range network order in glass, and, presumably alters its (longer range) morphology. Altogether, these findings imply that alkali mixing induces a chemical smoothening of vitrification [22], termed "strengthening" in Angell's classification of liquids [37].

At the same time, alkali mixing results in the non-additivity of the M–O interactions in glass [45-48]. Figure 10 compares the far-infrared spectra of typical mixed alkali glasses [48] with the linear combination of the corresponding end-member spectra. Such comparisons demonstrate that the high field strength cations in a mixed-alkali glass occupy more covalent sites than those occupied by the same cation in the single alkali glass. The opposite is observed for the low field strength cation [45,48]. The following structural picture emerges: In single alkali glasses, one kind of cation needs to compensate the structure by compromising its own bonding requirements with the constraints imposed by the network. It does that by occupying two distinct distributions of sites [41,42]. In mixed alkali glasses, the cation with the highest field strength can be more selective and assume mostly the high basicity sites, because the lower basicity sites can now be compensated by its weaker field strength counterpart.

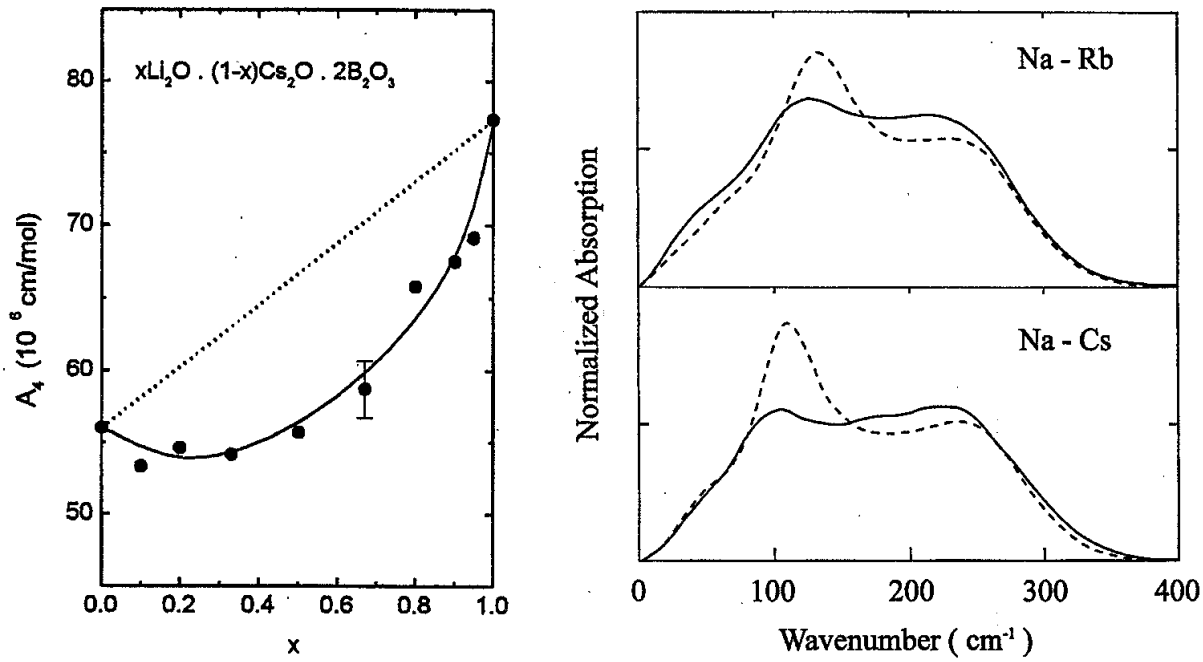

Fig. 9. (left) Integrated intensity of the infrared envelope due to $B\emptyset_4^-$ units in Li–Cs diborate glasses as a function of alkali mixing. Solid line is for guiding the eye, and the dotted line between end-members indicates additivity [45-47].

Fig. 10. (right) Far infrared spectra of Na–Rb and Na–Cs diborate glasses (solid line) compared to the weighted averages of their corresponding end-member spectra [45,48].

8. PERSPECTIVES

There is one conclusion that should be evident from the above discussion The chemical richness of borates can provide the keys to decode, on a structural basis, the complex and widespread phenomenon of vitrification. Everytime we study the structure of one particular glass composition, we ought to aim at unfolding the memory of those high-temperature processes that lead to its formation. The better we understand the potential energy hypersurface of a glass forming system, the easier we will discover how this system "flows" in it upon cooling. We need to map isomerizations, disproportionations and polymorphic transitions. Thus, we need to know more about crystalline borates. It is challenging to realize that most of the lithium borate compounds of a 1958 phase diagram [49] remain structurally unidentified. We also need to acquire more and direct evidence of the structure of borate melts, and on how this structure is affected by additives. We should understand the specific in order to be able to tackle the general. Once we adopt this perspective, new experimental techniques and theoretical approaches will develop. Among them, vibrational spectroscopy will keep playing an important role.

Acknowledgments

Data included in this report are due to the careful experimental work of M. A. Karakassides, A. P. Patsis, J. A. Kapoutsis, M. S. Bitsis and Y. D. Yiannopoulos (NHRF). Several of the ideas presented have benefited from discussions with J.

A. Duffy, M. D. Ingram, J. M. Hutchinson (Aberdeen), S. A. Feller (Coe), and H. Jain (Lehigh). We thank them all. Funding was provided by NHRF and occasionaly through European and international programmes.

REFERENCES

[1] C. A. Coulson & T. W. Dingle, *Acta. Cryst.* **B24** (1968), 153.
[2] J. Krogh-Moe, M. Ihara, *Acta Cryst.* **23** (1967), 27.
[3] A. Kirfel, G. Will & R. F. Stewart, *Acta Cryst.* **B39** (1983), 175.
[4] M. Marezio & J. P. Remeika, *J. Chem. Phys.* **44** (1966), 3348.
[5] H. Koenig, R. Hoppe & M. Jansen, *Z. anorg. allg. chem.* **449** (1979), 91.
[6] F. Stewner, *Acta Cryst.* **B27** (1971), 904.
[7] A. M. Heyns, K. J. Range & M. Wildenauer, *Spectrochim. Acta* **46A** (1990), 1621.
[8] P. Mondal & J. W. Jeffery, *Acta Cryst.* **B31** (1975), 689.
[9] G. D. Chryssikos, E. I. Kamitsos, A. P. Patsis & M. A. Karakassides, *Mater. Sci. Eng.* **B7** (1990), 1.
[10] C. T. Prewitt & R. D. Shannon, *Acta Cryst.* **B24** (1968), 869; A. Perloff & S. Block, *Ibid* **20** (1966), 274; D. L. Corker & A. M. Glazer, *Ibid* **B52** (1996), 260.
[11] E. I. Kamitsos & G. D. Chryssikos, *J. Molec. Struct.* **247** (1990), 1.
[12] E. I. Kamitsos, M. A. Karakassides & G. D. Chryssikos, *Phys. Chem. Glasses* **28** (1987), 203.
[13] G. D. Chryssikos, E. I. Kamitsos & M. A. Karakassides, *Phys. Chem. Glasses* **31** (1990), 109.
[14] E. I. Kamitsos, A. P. Patsis, M. A. Karakassides & G. D. Chryssikos, *J. Non-Cryst. Solids* **126** (1990), 52.
[15] G. E. Jellison, Jr., S. A. Feller & P. J. Bray, *Phys. Chem. Glasses* **19** (1978), 52.
[16] E. I. Kamitsos, A. P. Patsis & G. D. Chryssikos, *J. Non-Cryst. Solids* **152** (1993), 246.
[17] J. Zhong & P. J. Bray, *J. Non-Cryst. Solids* **111** (1989), 67.
[18] G. D. Chryssikos, *J. Raman Spectr.* **22** (1991), 645.
[19] G. D. Chryssikos, J. A. Kapoutsis, A. P. Patsis & E. I. Kamitsos, *Spectrochim. Acta* **47A** (1991), 1117.
[20] G. D. Chryssikos, J. A. Kapoutsis, M. S. Bitsis, E. I. Kamitsos, A. P. Patsis & A. J. Pappin, *Bol. Soc. Esp. Ceram. Vid.* **31-C2** (1992), 27.
[21] P. J. Bray, J. F. Emerson, Donghoon Lee, S. A. Feller, D. L. Bain & D. A. Feil, *J. Non-Cryst. Solids* **129** (1990), 283.
[22] G. D. Chryssikos, J. A. Kapoutsis, E. I. Kamitsos, A. P. Patsis & A. J. Pappin, *J. Non-Cryst. Solids* **167** (1994), 92.
[23] J. Krogh-Moe, *Acta Cryst.* **B30** (1974), 1178.
[24] S. Block & A. Perloff, *Acta Cryst.* **19** (1965), 297.
[25] J. Krogh-Moe, *Acta Cryst.* **B30** (1974), 578.
[26] N. L. Ross & R. J. Angell, *J. Solid State Chem.* **90** (1991), 27.
[27] R. W. Smith & D. A. Keszler, *Mater. Res. Bull.* **24** (1989), 725.
[28] J. Fayos, R. A. Howie & F. P. Glasser, *Acta Cryst.* **C41** (1985), 1396.
[29] W. Schneider & G. B. Carpenter, *Acta Cryst.* **B26** (1990), 1189.
[30] S. F. Radaev, L. A. Muradyan, L. F. Malakhova, Y. V. Burak & V. I. Simonov, *Sov. Phys. Crystalogr.* **34** (1989), 842.
[31] P. D. Thomson, J. Huang, R. W. Smith & D. A. Keszler, *J. Solid State Chem.* **95** (1991), 126.
[32] C. F. Windisch , Jr. & W. M. Risen, Jr., *J. Non-Cryst. Solids* **48** (1982), 307.
[33] J. Krogh-Moe, *Phys. Chem Glasses* **3** (1962), 101.
[34] W. L. Konijnendijk, *Philips Res. Rep. Suppl.* **1**, (1975), 1.
[35] G. D. Chryssikos, E. I. Kamitsos, A. P. Patsis, M. S. Bitsis & M. A. Karakassides, *J. Non-Cryst. Solids* **126** (1990), 42.
[36] G. D. Chryssikos, J. A. Duffy, J. M. Hutchinson, M. D. Ingram, E. I. Kamitsos & A. J. Pappin, *J. Non-Cryst. Solids* **172-174** (1994), 378.

[37] C. A. Angell, *J. Non-Cryst. Solids* **131-133** (1991), 13, and refs. therein.
[38] E. I. Kamitsos, *J. Phys. Chem.* **93** (1989), 1604.
[39] J. A. Duffy, G. D. Chryssikos & E. I. Kamitsos, *Phys. Chem. Glasses* **36** (1995), 53.
[40] G. D. Chryssikos, E. I. Kamitsos & Y. D. Yiannopoulos, *J. Non-Cryst. Solids* **196** (1996), 244.
[41] Y. D. Yiannopoulos, E. I. Kamitsos, G. D. Chryssikos & J. A. Kapoutsis, *Proc. Second Int. Conf. on Borates Glasses, Crystals and Melts*, 514.
[42] E. I. Kamitsos, M. A. Karakassides & G. D. Chryssikos, *Solid State Ionics* **28-30**, (1988) 687.
[43] E. I. Kamitsos, G. D. Chryssikos, A. P. Patsis & M. A. Karakassides, *J. Non-Cryst. Solids* **131-133** (1991), 1092.
[44] M. D. Ingram, *Phys. Chem. Glasses* **28** (1987), 215.
[45] E. I. Kamitsos, A. P. Patsis & G. D. Chryssikos, in *The Physics of Non-Crystalline Solids*, (L. D. Pye, W. C. LaCourse, H. J. Stevens, Eds), Taylor & Francis, London (1992), p. 460.
[46] E. I. Kamitsos, A. P. Patsis, G. D. Chryssikos & J. A. Kapoutsis, *Bol. Soc. esp. Ceram. Vid.* **31-C3** (1992), 287.
[47] E. I. Kamitsos, *J. Physique IV (Colloque)* **C4** (1992), 87.
[48] E. I. Kamitsos, A. P. Patsis & G. D. Chryssikos, *Phys. Chem. Glasses* **32** (1991), 219.
[49] B. S. R. Sastry & F. A. Hummel, *J. Am. Ceram. Soc.* **41** (1958), 7, and **42** (1959), 216.